

See discussions, stats, and author profiles for this publication at: <https://www.researchgate.net/publication/324520873>

Chirality dependence of electronic band structure and density of states in singlewalled carbon nanotubes

Article in *African Review of Physics* · April 2018

CITATIONS

5

READS

933

1 author:



Devi Dass

Government Gandhi Memorial Science College

22 PUBLICATIONS 128 CITATIONS

SEE PROFILE

Chirality dependence of electronic band structure and density of states in single-walled carbon nanotubes

¹Devi Dass*, and ²Rakesh Vaid

¹Department of Electronics, Govt. Degree College, Bhaderwah-182222, J & K, India

²Department of Electronics, University of Jammu, Jammu-180006, J & K, India

This paper investigates the role of chirality and its impact on the electronic band structure and the density of states in armchair and zigzag single-walled carbon nanotubes. Electronic band structures and the density of states for various chirality values has been analytically studied and verified using simulation approach. It has been observed that with the increase in chirality, the total number of bands in the electronic band structure gets increased and more Van Hove singularities appears in its density of states, which further increases the current capability of the CNTs. The analytical study of band gap and the density of states at Fermi energy ($E=0$) has been carried out and compared with the data obtained from simulations. The results suggest that the simulated values agree well with the analytical values thus validating the results. The paper also analytically verifies the metallic and semiconducting behavior of the single-walled CNTs.

1. Introduction

Carbon nanotubes (CNTs) have gained tremendous attention since these tubes were fabricated by various groups [1-3]. The way the graphite sheet is wrapped is represented by the chirality (n, m), which is an important parameter in designing a CNT. There is a need to investigate it further for the role it plays in the structure of a CNT [4]. If $n = m = l$, where l is an integer, the nanotube formed is known as armchair single walled (SW) CNT and if $n = l$ & $m = 0$, a zigzag SWCNT is formed, whereas for all other combinations of n and m give rise to a chiral carbon nanotube [5-6]. Wilder *et al* [7] further classified the CNTs and showed that a SWCNT with $n - m = 3l$, where l is zero or any positive integer are metallic and thus conducting with a fundamental gap of 0.0 eV. If the equation $n - m = 3l$ is not satisfied, the SWCNT behaves as a semiconductor with a fundamental energy gap with chirality (n, m), which can be calculated by the equation

$$E_g = \frac{2\gamma_0 a_{c-c}}{d_{(SWCNT)}} \quad (1)$$

where γ_0 (tight binding energy) and a_{c-c} (carbon-carbon spacing) are constants. The diameter of a SWCNT can be represented as a function of n and m are [4-6]

$$d_{(SWCNT)}(nm) = 0.0783\sqrt{n^2 + m^2 + nm} \quad (2)$$

Mathematically, the total number of bands in each electronic band structure depends on chirality (n, m) and can be calculated by the equation

$$N_{\text{bands}} = \frac{4(n^2 + m^2 + nm)}{\gcd(2n+m, 2m+n)} \quad (3)$$

where gcd stand for greatest common divisor. The electronic density of states in CNTs was studies by

Mintmire *et al* [8] in 1998 and the electronic behavior of SWCNTs was first observed using scanning tunneling microscopy by Wilder *et al* [7] and Odom *et al* [9] during 1998.

Later, the electronic density of states of SWCNTs have been characterized and compared with the results of (13, 7) and (12, 6) SWCNT obtained using tight binding calculation, which shows good agreement between experimental and tight binding calculations [10]. Ouyang *et al* [11] have confirmed in an experiment that the zigzag SWCNTs of chirality (9, 0), (12, 0) and (15, 0) have small band gaps from which they obtained a mathematical expression by fitting, but in our work these tubes show zero band gap.

Recently the band gaps and radii of metallic zigzag SWCNTs were calculated using density functional theory [12] and were compared with the results of Ouyang *et al* [11] but the effect of chirality on SWCNT performance has not been discussed in any of the research papers published so far.

This paper investigates the chirality dependence in armchair and zigzag SWCNTs on their electronic band structure and the density of states, which subsequently verifies the metallic and semiconducting behavior of SWCNTs.

2. Analytical Expressions for Electronic Band Structure of SWCNTs

In this section, we have derived the electronic band structure for CNTs from graphene band structure. To proceed, we start from the derivation of 2D electronic band structure of graphene which can be expressed as [13]

$$E(k) = E(k_x, k_y) = \pm \gamma_0 \left[1 + 4\cos\left(\frac{\sqrt{3}k_x a}{2}\right) \cos\left(\frac{k_y a}{2}\right) + 4\cos^2\left(\frac{k_y a}{2}\right) \right]^{-\frac{1}{2}} \quad (4)$$

where k_x and k_y are the x and y components of the wave vector k , $\gamma_0 \approx 2.7$ eV is the overlap energy for C-C bond and $a = 0.246$ nm is the graphite lattice constant. The negative sign in Eqn. (4) denotes valence bands of graphene formed by bonding π orbitals while the positive sign in Eqn. (4) denotes conduction bands of graphene formed by antibonding π^* orbitals. At temperature equal to 0K, all of the electrons occupy the lower π band and the upper π^* band is empty.

The electronic band structure of a CNT can be obtained from the electronic band structure of graphene by quantizing the wave vector k along the circumferential direction of carbon nanotubes. If we consider a CNT as an infinitely long cylinder, there are two wave vectors associated with it. The wave vector k_{\parallel} which is parallel to CNT axis and is continuous while the wave vector k_{\perp} , which is along the circumference of a CNT, should satisfy a periodic boundary condition

$$k_{\perp} C_h = \pi d_{\text{(SWCNT)}} k_L = 2\pi p \quad (5)$$

where $d_{\text{(SWCNT)}}$ is the diameter of a SWCNT and p is an integer.

As a result, each band of graphene splits into a number of 1-D sub-bands labeled by p . This boundary condition leads to quantized values of allowed k_{\perp} for SWCNTs. Then, the 1D band structure of SWCNTs can be obtained from cross-sectional cutting of the band structure of 2D graphene with these allowed k_{\perp} states. This is called zone- folding scheme of obtaining the band structure [14-17].

2.1 Derivation for Electronic Band Structure of armchair SWCNT

$$E(k_y) = \pm \gamma_0 \left[1 + 4\cos\left(\frac{\pi p}{l}\right) \cos\left(\frac{k_y a}{2}\right) + 4\cos^2\left(\frac{k_y a}{2}\right) \right]^{-\frac{1}{2}} \quad (7)$$

where $(-1 \leq k_y \leq 1)$ and the index p takes the values $p = 0, 1, 2, 3, 4, 5, \dots, [\frac{N_{A\text{-bands}}}{2} - 1]$. $N_{A\text{-bands}}$ are the number of bands in electronic band structure of armchair SWCNT. Each band structure of armchair SWCNT yield $4l$ energy sub-bands with $2l$ conduction and $2l$ valence bands and of these $2l$ bands, two bands are non-degenerate and $l-1$ are doubly degenerate. The sub-bands obtained for $p = \pm 0$ & $\pm l$ are non-degenerate and doubly degenerate for other values of p . The degeneracy comes from the two sub-bands with the same energy dispersion, but different p -values.

An armchair SWCNT has chirality $(n, m) = (l, l)$, where l is an integer. In this SWCNT, the tube axis is parallel to y -direction and the circumference represents the x -direction (Fig. 1). Since the circumference of armchair SWCNT is

$$\begin{aligned} C_h &= a\sqrt{n^2 + m^2 + nm} \\ &= a\sqrt{l^2 + l^2 + l^2} = \sqrt{3}la \end{aligned}$$

So, $C_h = \sqrt{3}la\hat{x}$

Therefore, the periodic boundary condition (Eqn. (5)) then becomes

$$\begin{aligned} k_x C_x &= 2\pi p; \\ k_x \sqrt{3}la &= 2\pi p; \\ k_x &= \frac{2\pi p}{\sqrt{3}la} \end{aligned} \quad (6)$$

After putting the values of p and l in equation (6), we see that the allowed values of k_x lie parallel to the k_y -axis (as shown in Fig. 1). It can also be seen from Fig. (1) that the lines of quantized circumferential wave vector k_x intersect the graphene Fermi points, therefore, the armchair SWCNT is metallic with no bandgap.

Again, by putting the values of k_x from equation (6) to equation (4), we get the 1D band structure of armchair SWCNT and can be calculated as

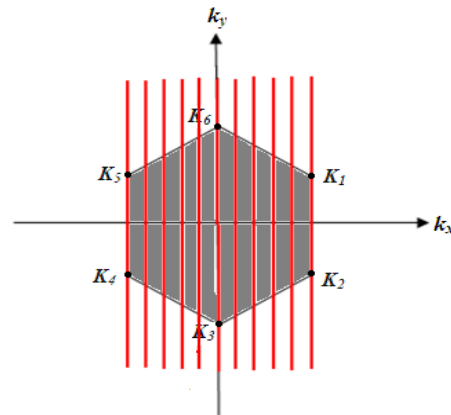


Fig.1 2D First Brillouin zone of graphene and allowed wave vector lines shows metallic behavior of armchair SWCNT.

2.2 Derivation for Electronic Band Structure of zigzag SWCNT

A zigzag SWCNT has chirality $(n, m) = (l, 0)$ where l is an integer. In this SWCNT, the tube axis is parallel to x -direction and the circumference represents the y -direction. Since the circumference of zigzag SWCNT is:

$$C_h = a\sqrt{n^2 + m^2 + nm} \\ = a\sqrt{l^2 + 0^2 + 0.0} = la$$

So, $C_h = la\hat{y}$

Therefore, the periodic boundary condition (Eqn. (5)) then becomes

$$k_y C_y = 2\pi p;$$

$$k_y la = 2\pi p;$$

$$k_y = \frac{2\pi p}{la} \quad (8)$$

By choosing the value of p and l , we see that the allowed values of k_y lie parallel to the k_x -axis as shown in Fig. (2) where the first Brillouin zone of graphene is shown as a shaded hexagon with the Fermi points at the six corners. In Fig. 2(a), the lines of quantized circumferential wave vector k_y intersect the graphene Fermi points, which means that the zigzag SWCNT is metallic without a band gap, whereas in Fig. 2(b) the lines of quantized circumferential wave vector k_y do not intersect the graphene Fermi points, which means that the zigzag SWCNT is semiconducting with a band gap.

By putting the values of k_y from Eqn. (8) to eqn. (4), we get the 1D band of structure zigzag SWCNT and can be calculated as:

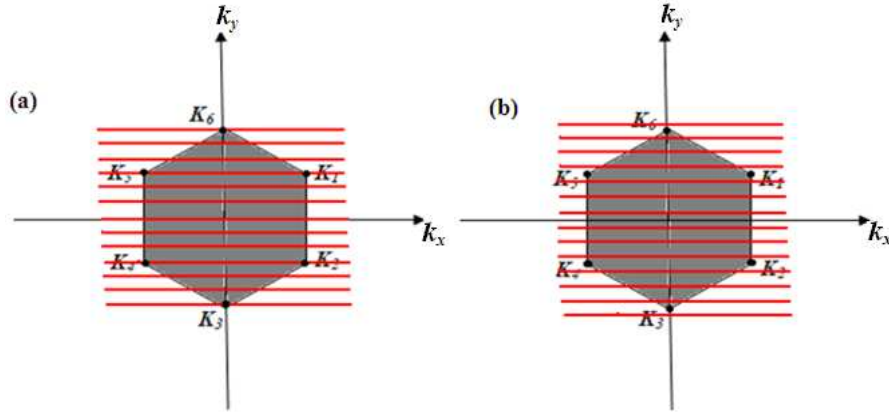


Fig. 2 2D First Brillouin zone of graphene and allowed wave vectors lines leading to (a) metallic zigzag SWCNT (b) semiconducting zigzag SWCNT.

$$E(k_x) = \pm \gamma_0 \left[1 + 4\cos\left(\frac{\sqrt{3}k_x a}{2}\right) \cos\left(\frac{\pi p}{l}\right) + 4\cos^2\left(\frac{\pi p}{l}\right) \right]^{-\frac{1}{2}} \quad (9)$$

where $(-1 \leq k_x \leq 1)$ and index p takes the values $p = 0, 1, 2, 3, 4, 5, \dots, \left[\frac{N_{Z-bands}}{2} - 1\right]$. $N_{Z-bands}$ are the number of bands in electronic band structure of zigzag SWCNT.

3. Results and Discussion

In this section, we have discussed the effect of chirality of armchair and zigzag SWCNTs on their electronic band structures and density of states simulated using p_z orbital tight binding method.

These results are obtained from the nanohub simulator CNT Bands [18] in which the chirality (n, m) of the tube is varied while the tight binding energy (3eV), carbon-carbon spacing (0.142nm), length of nanotube (5nm) are fixed parameters.

3.1 Effect of chirality on electronic band structure in armchair SWCNT

The electronic band structures of armchair SWCNT for chiralities: $n = m = 1, 2, 3, 4, 5, 6, 7, 8, 9, 10, 11$ and 12 as shown in Fig. (3). Each electronic band structure is symmetric, that is, $E(k_y) = E(-k_y)$ and describes the energy-momentum relationship for carriers within the first Brillouin zone. Each

continued line is an allowed level of energy for carriers or a sub-band. The sub-band closest to the equilibrium Fermi level ($E = 0$) is of particular interest, since they are usually the levels giving rise to current. The dashed lines sub-bands are non-degenerate bands, whereas the solid lines sub-bands are degenerate bands. The degeneracy comes from the two sub-bands with the same energy dispersion. Therefore, in each band structure of armchair SWCNT, the upper and lower conduction as well as valance bands are non-degenerate while other bands are doubly degenerate.

It can be also seen from the Fig. (3) that with the increase in chirality in armchair SWCNT by 1, the total number of bands in its electronic band structures increases by 4, which further indicates that the number of carriers increases so that the current capability of armchair CNT increases. Also, in each electronic band structure of armchair SWCNT, the upper valance band and lower conduction band cross each other at Fermi energy ($E = 0$), therefore, each armchair SWCNT exhibits metallic behavior.

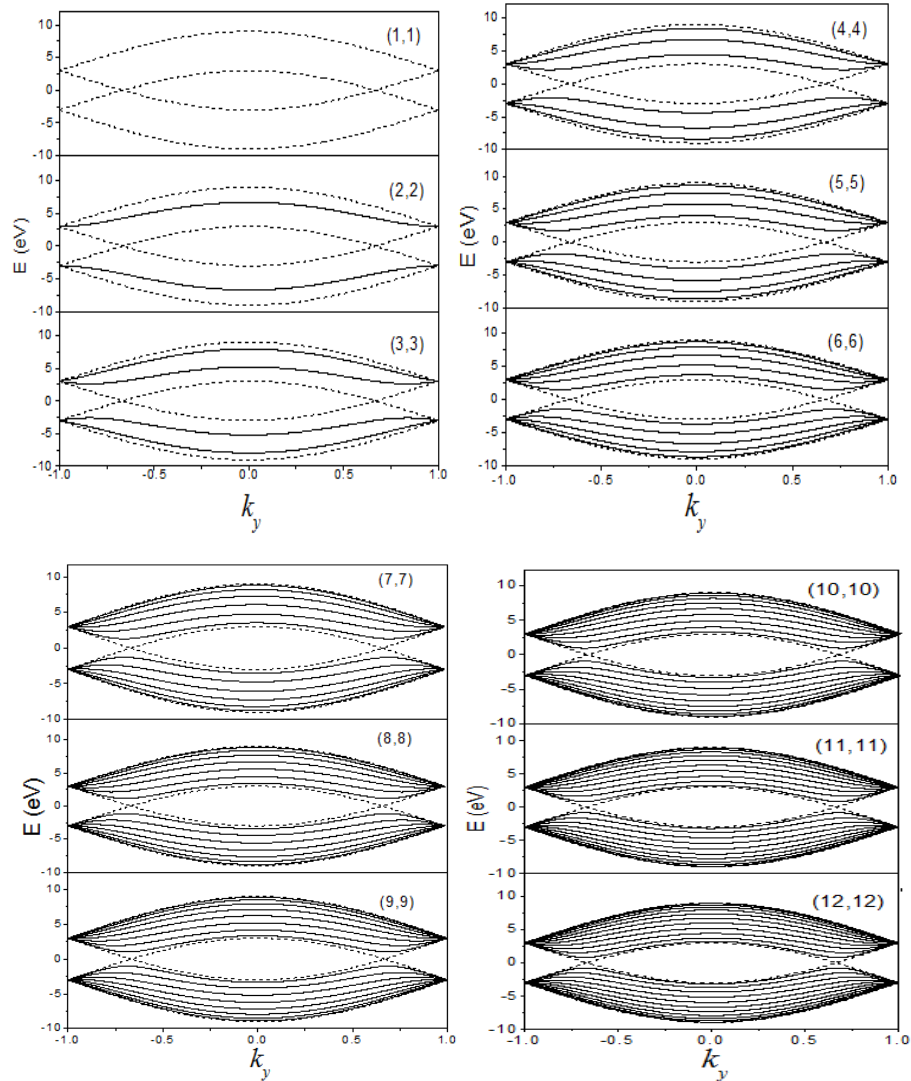


Fig. 3 Electronic band structures of armchair CNT for different chirality values.

The validation of simulated electronic band structures in armchair SWCNT. In general, an armchair SWCNT has chirality ($n = m = l$). By putting this chirality value in Eqn. (3), the total number of bands in each band structure is $N_{A\text{-bands}} = 4l$. Now, for $l = 1, 2, 3, 4, 5, 6, 7, 8, 9, 10, 11$, and

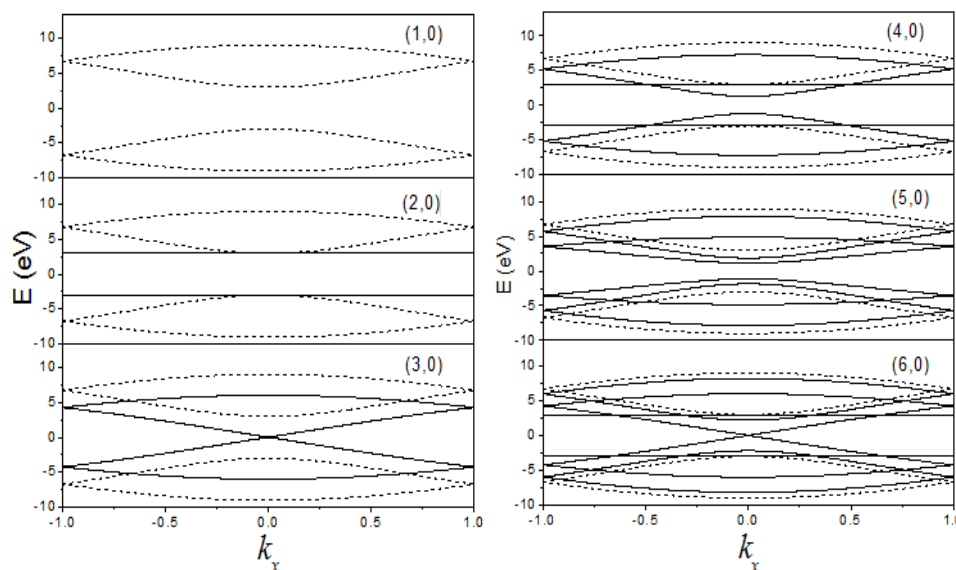
12, that is, for $(n, m) = (1, 1), (2, 2), (3, 3), (4, 4), (5, 5), (6, 6), (7, 7), (8, 8), (9, 9), (10, 10), (11, 11)$ and $(12, 12)$ we get, the total number of bands for these chirality values = 4, 8, 12, 16, 20, 24, 28, 32, 36, 40, 44, and 48. Hence, mathematically, we can say that with the increase in the chirality $(n, m) = (l,$

l) in armchair SWCNT by 1 and the total numbers of bands in its electronic band structure are increased by 4. For each chirality value, the equation $n - m = 3p$, where p is an integer, is satisfied. It means all armchair SWCNTs shows metallic behavior with zero band gap. Further, each electronic band structure of armchair SWCNT satisfies Eqn. (7). Hence, the simulated description of electronic band structures in armchair SWCNT match very well with mathematical description thus validating, both the simulations as well as analytical description.

3.2 Effect of chirality on electronic band structure in zigzag SWCNT

The electronic band structures in zigzag CNT for chirality $n = 1, 2, 3, 4, 5, 6, 7, 8, 9, 10, 11$, and 12 are shown in figure 4. It can be seen here that each electronic band structure is different from electronic band structure of armchair SWCNT (figure 3) but the number of bands in its electronic band structures are the same in armchair electronic band structures,

that is, with the increase in chirality value n in the zigzag CNT by 1, the number of bands in its electronic band structure also increases by 4. In the electronic band structure of (3, 0), (6, 0), (9, 0) and (12, 0) zigzag SWCNTs, the upper valance band and lower conduction band cross each other at Fermi energy ($E = 0$) and it shows metallic behavior. For electronic band structures of chiral values (1, 0), (2, 0), (4, 0), (5, 0), (7, 0), (8, 0), (10, 0), and (11, 0) of zigzag SWCNT, there is a gap between upper valance and lower conduction band and show semiconducting behavior. As the chirality of the semiconducting zigzag CNT increases, the gap between upper valance and lower conduction band decreases, which further indicates that the energy required to move the electrons from valance band to conduction band decreases and which in its turn increases the current capability of semiconducting zigzag SWCNT. In all the electronic band structures of zigzag SWCNTs, the upper valance and lower conduction bands are doubly degenerate.



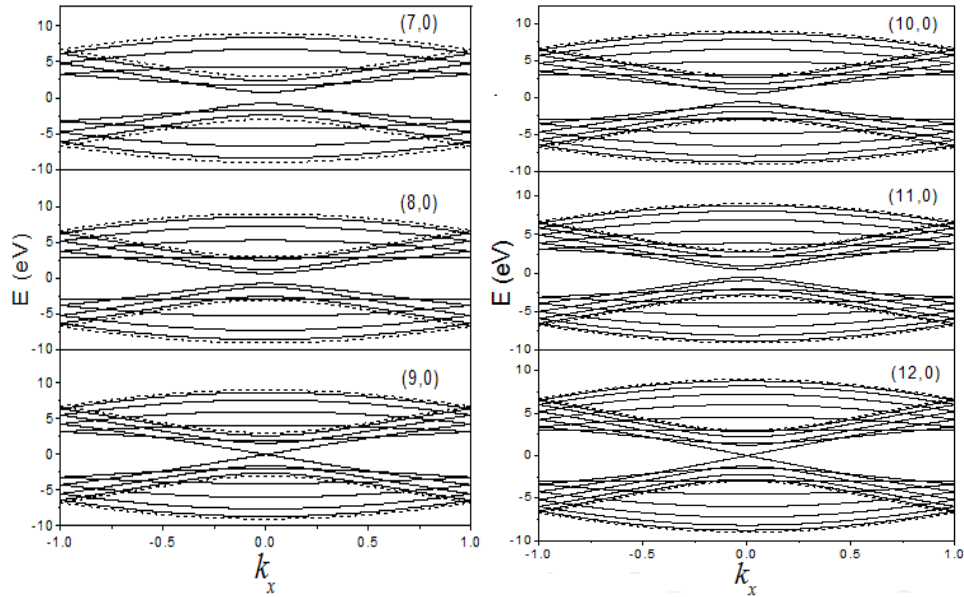


Fig. 4 Electronic band structures of zigzag single-walled CNT for different chirality values.

Validation of simulated electronic band structure in zigzag SWCNT. In general, a zigzag CNT has chirality $(n = l, m = 0)$. By putting this chirality value in Eqn. (3), the total number of bands in each band structure are $N_{\text{bands}} = 4l$. For $l = 1, 2, 3, 4, 5, 6, 7, 8, 9, 10, 11$, and 12 , that is, for $(n, m) = (1, 0), (2, 0), (3, 0), (4, 0), (5, 0), (6, 0), (7, 0), (8, 0), (9, 0), (10, 0), (11, 0)$ and $(12, 0)$, the total number of bands for these chiral values of zigzag SWCNTs are $4, 8, 12, 16, 20, 24, 28, 32, 36, 40, 44$, and 48 . Hence, mathematically, we can say that with the increase in the chirality $(n, m) = (l, 0)$ in a zigzag SWCNT by 4 , the total number of bands in its electronic band structure is increased by 4 . For

chiral values $(3, 0), (6, 0), (9, 0)$ and $(12, 0)$, the zigzag SWCNT shows metallic behavior because it satisfies the equation $n - m = 3p$ where p is an integer. For chiral values $(1, 0), (2, 0), (4, 0), (5, 0), (7, 0), (8, 0), (10, 0)$, and $(11, 0)$, the zigzag SWCNTs show semiconducting behavior because equation $n - m = 3p$ is not satisfied. Each electronic band structure in zigzag SWCNT satisfies equation (9). The band gap of semiconducting zigzag SWCNT is inversely related to its chirality as the diameter is directly related to chirality. Hence, the simulated description of electronic band structures of zigzag SWCNT match very well with mathematical description thus validating, both the simulations as well as analytical description.

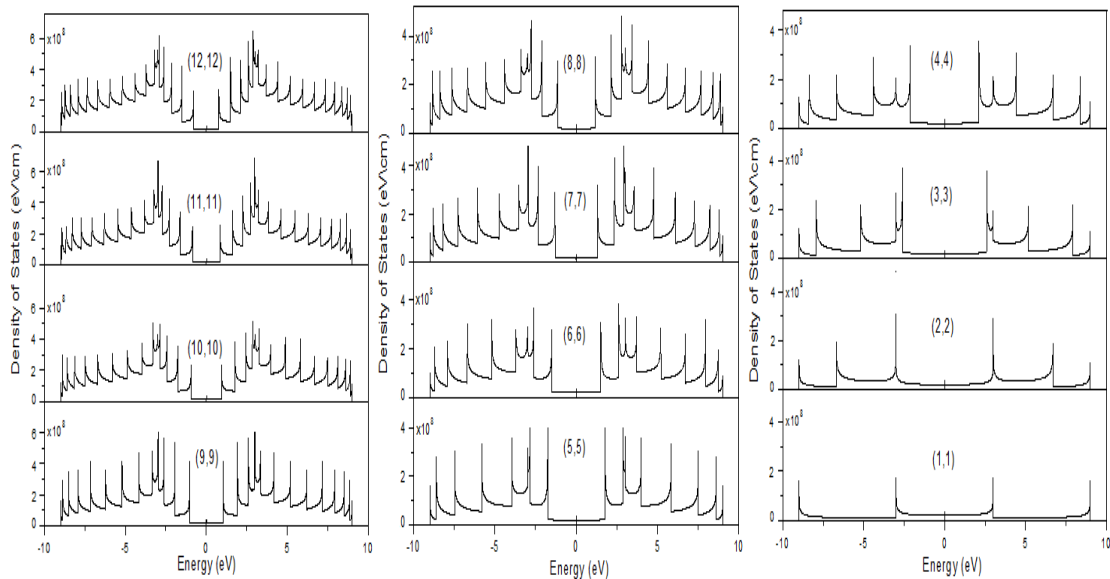


Fig. 5 Electronic density of states of armchair CNT for different chirality values.

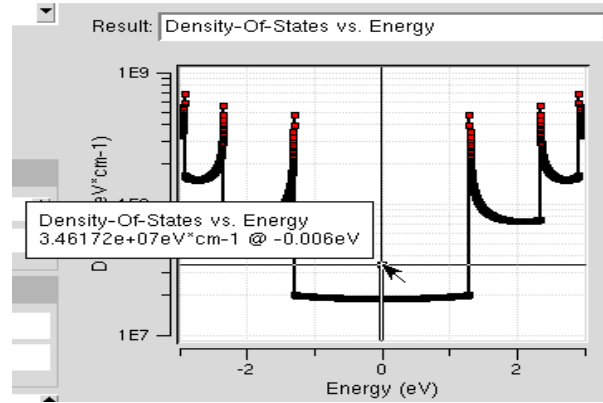


Fig. 6 Simulated density of states of armchair SWCNT.

3.3 Effect of chirality on electronic density of state in armchair SWCNT

Electronic density of states in armchair SWCNTs for chirality values $n = m = 1, 2, 3, 4, 5, 6, 7, 8, 9, 10, 11$, and 12 are shown in Fig. 5. Each electronic density of state tells us about the number of allowed states at certain energy. Each state can accommodate up to 2 electrons having different spins. This is Pauli's exclusion principle. At the Fermi energy ($E \approx 0$), the density of state is finite in each diagram, which means that all armchair SWCNTs are metallic in nature. Sharp peaks in the density of states, called Van Hove singularities, appear at specific energy levels. Further it can be seen from Fig. (5) that as the chirality of the armchair SWCNT is increased; numbers of sharp peaks in the density of states are observed which means more electronic states are available for

current conduction. If we write v_1, v_2, v_3, \dots are the Van Hove singularities in the valance band and c_1, c_2, c_3, \dots are the Van Hove singularities in the conduction band, then the transition from v_1 to c_1 (first symmetric van hove singularities) is around 3eV for the (1, 1) armchair SWCNT. This transition from v_1 to c_1 decreases as the chirality of the armchair SWCNT increases. The simulated value of density of states at $E \approx 0$ (Fig. (6)) is $3.46172e + 07$ eV/cm for each chirality in armchair SWCNT. Mathematically, the density of states at $E \approx 0$ can be calculated [19] as

$$D(E \approx 0) = \frac{8}{\sqrt{3}\pi\gamma_0 a_{c-c}} = \frac{8}{\sqrt{3} \cdot 3.14 \cdot 3eV \cdot 0.142 \cdot 10^{-9}m}$$

$$= 3.44e + 07 \text{ (eV*cm)}^{-1}, \text{ which is 0.02 times less than the simulated value. Hence, the simulated values of density of states at Fermi energy are in good agreement with the calculated values.}$$

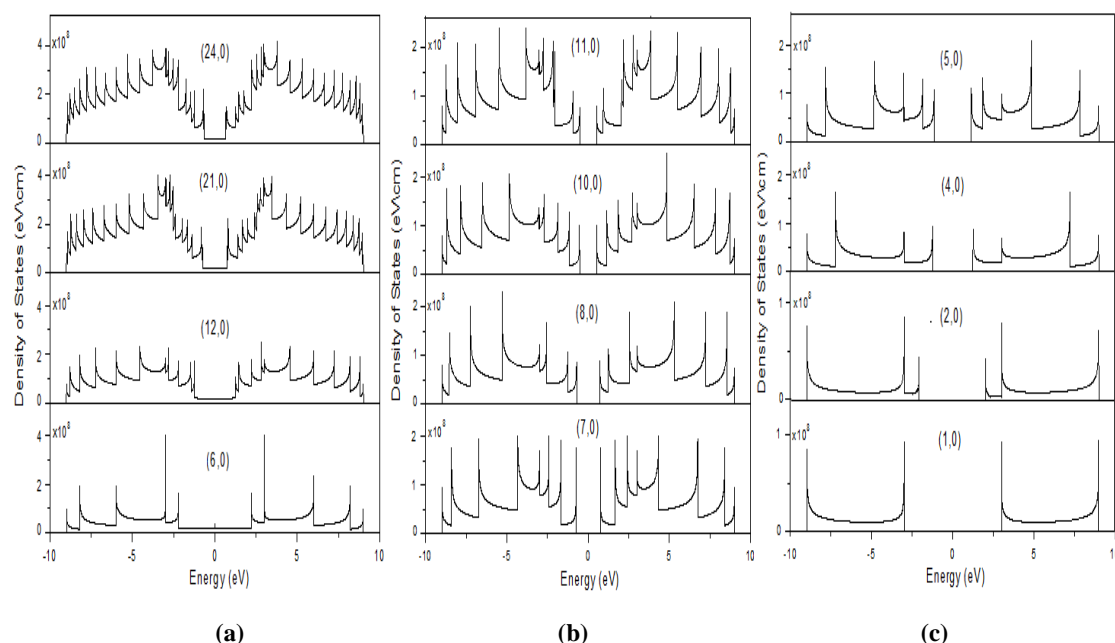


Fig. 7 Electronic Density of States of zigzag single-walled CNT for different chiralities

3.4 Effect of chirality on density of states in zigzag SWCNT

Electronic density of states in zigzag SWCNTs for chirality values $n = 1, 2, 4, 5, 6, 7, 8, 10, 11, 12, 21$ and 24 are shown in Fig. 7. It has been observed that for chiralities $(6, 0)$, $(12, 0)$, $(21, 0)$ & $(24, 0)$, the value for density of state is finite at Fermi energy ($E \approx 0$), which indicates that these zigzag SWCNTs show metallic behavior [see Fig. 7(a)].

For chirality values $(1, 0)$, $(2, 0)$, $(4, 0)$, $(5, 0)$, $(7, 0)$, $(8, 0)$, $(10, 0)$, & $(11, 0)$, there is a zero value for density of states at Fermi energy ($E \approx 0$), which indicates the semiconducting behavior (see Figs. 7(b) and 7(c)). In Fig. 8(b) and 8(c), it can also be

seen that the energy required to move the electrons from valance states to conduction states (called band gap denoted by E_g) decreases with the increase in chirality, which further indicates that the current capability of semiconducting zigzag SWCNTs increase. Therefore, this feature of semiconducting zigzag SWCNT can be useful for high performance MOSFET applications. Further, the comparison of simulated and calculated band gap of zigzag SWCNT is also shown in Table 1 indicating good agreement. For each metallic zigzag SWCNTs, the simulated value for density of states at ($E \approx 0$) [figure (8)] is $3.60283e + 07$ while the calculated density of states at ($E \approx 0$) is $3.44e + 07$, which is 0.16 times smaller than the simulated value

Table 1 Comparison of simulated with calculated band gap of semiconducting zigzag CNT

Zigzag chirality ($n = l, m = 0$)	Simulated band gap [18]	Calculated band gap (eq. 1)
(1, 0)	6 eV	10.881 eV
(2, 0)	4 eV	5.440 eV
(3, 0)	0 eV	0 eV
(4, 0)	2.4853 eV	2.720 eV
(5, 0)	2.2918 eV	2.176 eV
(6, 0)	0 eV	0 eV
(7, 0)	1.4819 eV	1.554 eV
(8, 0)	1.4078 eV	1.360 eV
(9, 0)	0 eV	0 eV
(10, 0)	1.0534 eV	1.088 eV
(11, 0)	1.0150 eV	0.989 eV
(12, 0)	0 eV	0 eV

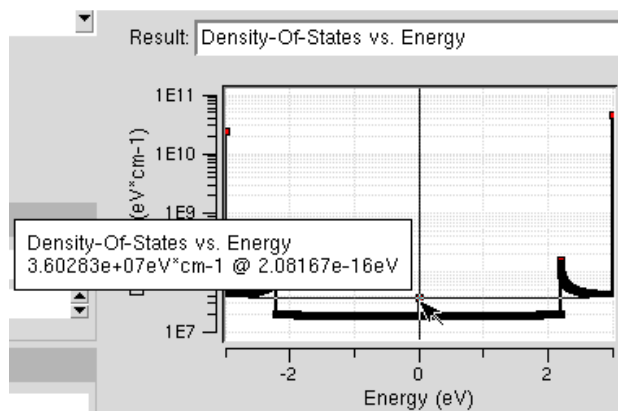


Fig. 8 Simulated density of states of metallic zigzag SWCNT

4. Conclusions

Impact of changing chirality in armchair and zigzag single-walled CNT on electronic band structures and density of states has been studied. It has been verified analytically that with the increase in chirality both in armchair and zigzag single-walled CNTs by 1, the total number of sub-bands in their electronic band structure increase by 4. It has been further verified analytically as well as by simulations that all armchair SWCNTs shows metallic behavior, whereas zigzag SWCNTs shows both metallic as well as semiconducting behavior. Finally, it has been concluded that the metallic SWCNTs are useful for interconnects and semiconducting SWCNTs are useful for electronic devices.

References

- [1] S. Iijima, "Helical microtubules of graphitic carbon", *Nature*, vol. 354, pp. 56-58, 1991.
- [2] S. Iijima, and T. Ichlhashi, "Single-shell carbon nanotubes of 1 nm diameter", *Nature*, vol. 363, pp. 603-605, 1993.
- [3] D.S. Bethune, C.H. Kiang, M.S. Devries, G. Gorman, R. Savoy, J. Vazquez, and R. Beyers, "Cobalt-catalyzed growth of carbon nanotubes with single-atomic-layer walls", *Nature*, vol. 363, pp. 605-607, 1993.
- [4] D. Dass, R. Prasher, and R. Vaid, "Analytical study of unit cell and molecular structures of single walled carbon nanotubes", *International Journal of Computational Engineering Research*, vol. 2, pp. 1447-1457, 2012.
- [5] M.S. Dresselhaus, G. Dresselhaus, and R. Saito, "Physics of carbon nanotubes", *Carbon*, vol. 33, pp. 883-891, 1995.
- [6] H. R. Tabar, "Computational physics of carbon nanotubes", Cambridge University Press, New York, 2008.
- [7] J. W. G. Wilder, L. C. Venema, A. G. Rinzier, R. E. Smalley, and C. Dekker, "Electronic structure of atomically resolved carbon nanotubes", *Nature*, vol. 391, pp. 59-62, 1998.
- [8] J. W. Mintmire, and C. T. White, "Universal density of states for carbon nanotubes", *Physical Review Letters*, vol. 81, pp. 2506-2509, 1998.
- [9] T. W. Odom, J. L. Huang, P. Kim, and C. M. Lieber, "Atomic structure and electronic properties of single-walled carbon nanotubes", *Nature*, vol. 391, pp. 62-64, 1998.
- [10] P. Kim, T. W. Odom, and C. M. Lieber, "STM study of single-walled carbon nanotubes", *Carbon*, vol. 38, pp. 1741-1744, 2000.
- [11] M. Ouyang, J. L. Huang, C. L. Cheung, and C. M. Lieber, "Energy gaps in metallic single-walled carbon nanotubes", *Science*, vol. 292, pp. 702-705, 2001.
- [13] R. Wan, J. H. Peng, X. Zhang, and C. Leng "Band gaps and radii of metallic zigzag single wall carbon nanotubes", *Physica B*, vol. 417, pp. 1-3, 2013.
- [14] P. R. Wallace, "The band theory of graphite", *Physical Review Letters*, vol. 71, pp. 622-634, 1947.

- [15] E. D. Minot, “Tuning the band structure of carbon nanotubes”, Ph. D. Thesis, Cornell University, 2004.
- [16] A. Verma, “Theoretical and numerical studies of semiconducting carbon nanotubes”, Ph. D. Thesis, Department of electrical engineering, Georgia Institute of Technology, 2006.
- [17] F. Leonard, “The physics of carbon nanotube devices”, William Andrew, New York, 2008.
- [18] A. Javey, and J. Kong, “Carbon nanotube electronics”, Springer, New York, 2009.
- [19] G. Seol, Y. Yoon, J. K. Fodor, J. Guo, A. Matsudaira, D. Kienle, G. Liang, G. Klimeck, M. Lundstrom, and A. I. Saeed, “CNTbands”, 2010.
- [20] X. Liu, “Synthesis, devices and applications of carbon nanotubes”, Ph. D. Thesis, University of Southern, California, 2006.

Received: 03 March, 2017

Accepted: 27 March, 2018